Whites Science
A Scientific Erudition

ADSORPTION OF RARE GAS ATOMS ON Cu (111) SURFACE

Koushiki Gupta and Asoke P. Chattopadhyay*
Department of Chemistry, University of Kalyani, Kalyani 741235, India

ABSTRACT

Adsorption of rare-gas atoms on a three layer model of Cu(111) surface was studied at the DFT level with two different functionals. The binding energy values increase from He to Ar, then decreases somewhat to Kr. For He, atop atom site seems most favourable, for others it is the bridge site. Bond distances change little from He to Kr, and for binding sites. Various other molecular parameters such as dipole moment, HOMO and LUMO energies, charges on various moieties, electronegativity and electrophilicity values are shown as function of adsorbate-metal distance. Density of states (DOS) plots also show effect of rare-gas atoms.

Keywords : Adsorption, rare-gas atom, Cu(111) surface, DFT, functionals

INTRODUCTION

The type of interaction of the nature of rare-gas adsorption on transition metal surfaces is a typical example of weak physical adsorption. The van der Waals (vdw) type interaction involved in this phenomenon is not as simple to explain as in the case of rare-gas clusters. Close approach of a rare gas atom towards the surface of any metal surface invokes chemical interaction. At long distances, the formation of layers on the metal surface is governed by attractive vdw forces along with Pauli repulsion restricting the distance of closest approach and thus leading to a distinct potential minimum. Thus, at large separations, the mechanism of the layer formation is same as that observed for rare-gas condensation. The chemical contribution arising at closer distances contributes towards the attraction part. The nature of the potential expected at longer separation is thus modified as the rare gas atoms approach the metal surface more closely. The simple vdw type interaction between the surface and the atoms has to be investigated in detail keeping in mind the chemical interaction involved in the process. Thus, it can be summarised that the interaction of a noble gas with a surface results from the balance between the vdw attraction, the Pauli repulsion and depending on the nature of the substrate, induced electrostatic interactions. We present a detailed study of the nature of potentials obtained due to the interaction of rare gas atoms with some particular metal surfaces.

From the early days of surface science, the above type of chemical interactions in the metal surface-rare gas interface have received considerable attention[1]. One of the significant results of early times was published by Lang[2]. The relationship between the vdw description of the binding of rare gas atoms to metal surfaces was studied using a local approximation for exchange correlation effects and a good account was obtained of various physical properties. Physisorbed monolayers of rare gas atoms adsorbed on smooth clean single crystal substrates have been subject of extensive research in the recent years[3] as they represent the simplest experimental representation of quasi two-dimensional model systems. This interest was increased by the development of rare-gas scattering as a technique for studying the structural characteristics of clean and adsorbate-covered surfaces[4]. It was assumed[5] that the rare gases were preferentially bound at high coordination sites on the surface, and the net interaction between adsorbed rare gas atoms would be attractive. However, on the other hand, it was also found that Xe atoms formed a stable dilute phase even at very low temperatures on low indexed Pd surfaces, which indicates a repulsive interaction between the Xe atoms adsorbed on Pd[6-8] . The interaction of xenon with metallic substrates in particular has been widely studied, both theoretically and experimentally[2, 9-12] . For metal-atom adsorption on metal surfaces at low temperatures little motion is observed for adsorbing

*Corresponding author:
Email: asoke@klyuniv.ac.in

http://dx.doi.org/10.20530/IJIBCS_8_1-12
ISSN 2047-9093 © 2016

atoms[13-14]. But for Xe on Pt(111) the motion allows the adsorbing atom to find the lowest energy adsorption sites such as steps and surface defects and to form compact islands. It can be concluded that the Xe atoms preferentially bind to step edges on the Pt (111) surface. On the other hand, studies of Xe adsorption with non metallic surfaces are scarce with the exception of the graphite which due to its inertness, has been widely used as a substrate for physisorption studies. In an impressive series of experiments, Webb and coworkers[15-17] have been able to show that the properties of adsorbed monolayers of Xe, Kr and Ar on Ag(111) to a good approximation can be described by assuming a laterally uniform holding substrate potential. Black and Bopp[18] have recently investigated the Xe/Pt(111) system by molecular dynamics techniques but their results were not well reproduced. A few other studies of the monolayer of xenon adsorbed on the (111) face of platinum were presented in these studies[19-24] .

A different case where noble gas adsorption on non-metallic surfaces has raised considerable interest involves the rutile polymorph of titanium dioxide (TiO_2). Recently Ar adsorption on rutile has been studied from experimental[25-27] and theoretical point of view[28]. In a report by Gomes[29], the effect of larger polarisability and larger atomic size of adsorbate rare gas atom were inspected by a density functional study of the interaction of Xe with TiO_2(110). The Xe atom is found to have a deeper physisorption well on a defect-free substrate when compared with their previous study with Ar[28] . A series of theoretical works have been performed for monolayer of Xe/Pt(111) by Black and co-workers[30-33] **.** Bethune, Barker and Rettner[34] constructed a Xe-Pt potential by attributing a small vdw radius to the Xe atom. Tully and co-workers performed a series of calculations on the Xe-Pt potential[35-37]. Hall et al.[38] modelled the frequency spectrum of incommensurate mono-, bi- and tri-layers of inert gases on Pt (111) using conventional models for adatom-adatom interactions. The use of pair potentials deduced from gas-phase data provided an adequate description of the lateral interactions between adsorbates. In a series of studies, Gottlieb[39-40] studied uniaxial incommensurate structures of a rare gas monolayer physisorbed on a triangular Bravais surface lattice for Xe/Pt(111) system and interpreted the previous experimental results as showing the positioning of the Xe atoms in the commensurate lattice to be the atop sites rather than the three-fold sites. Eigler, Weiss and Schweizer[41] obtained images of individual Xe atoms on a Ni (110) surface using a low temperature scanning tunnelling microscope. Pothoff et al[42-43] studied spin polarised low energy diffraction studies on Xe/Pt (111) and showed strong contribution from multiple scattering between the substrate and the adlayer. It was found that the Xe atoms were adsorbed in the domains of fcc and hcp hollow sites of the Pt (111) surface. Perez et al.[44] presented short range interaction between the Xe atoms and different adsorption sites for Xe and various metal systems. They showed that the chemical interaction between the Xe and the metal orbitals accounts for as much as half the adsorption energy and thus it cannot be neglected.

MATERIALS AND METHODS

A three layer cluster model was designed to represent Cu (110) surface (see below). It consists of 10 top layer atoms, 7 second layer and 9 third layer atoms. All interactions with rare gas atoms were limited to specific locations on this cluster viz. atop-atom, bridge, 3-fold hollow (no 3rd layer copper atom beneath it)and 3-fold filled sites (with a Cu atom directly under it). Final DFT calculations were performed with a GGA functional, PW91[45] and a hybrid functional, B3LYP[46] after testing with some other functionals such as PBE[47] etc. We made use of the single valence basis sets[48] for the calculation and the lattice parameter used for copper was optimised to 3.6149 A. The entire calculation was performed using ORCA 2.7 software suite[49] .

RESULTS AND DISCUSSION

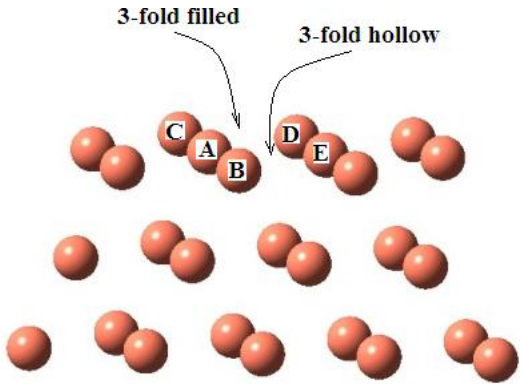

Fig. 1. The 26 atom 3-layer cluster model used in this study. 3-fold filled and hollow sites are varied from the surface. The binding energy and various other physical properties for such interactions are presented in this study.

Table 1. Equilibrium distance and binding energy data for for rare gas atoms on Cu(111) cluster model for different binding sites (A = atop atom, B = bridge site, F = 3-fold filled site, H = 3-fold hollow site)

	Equilibrium distance (Å)								Binding energy (mEV)							
	B3LYP				PW91				B3LYP				PW91			
	A	B	F	H	A	B	F	H	A	B	F	H	A	B	F	H
He	3.6	3.7	3.8	4.0	3.4	3.5	3.4	3.4	24.9516	22.5027	18.1497	21.6864	74.3116	71.0462	71.5904	68.8693
Ne	3.4	3.5	3.5	3.5	3.5	3.3	3.3	3.3	84.8136	95.4255	88.6230	94.8813	148.7918	167.5677	158.0437	160.2206
Ar	4.0	3.9	4.0	4.0	3.7	3.7	3.8	3.7	117.1935	129.4380	116.9105	119.9145	191.7967	208.6678	202.1371	201.0486
Kr	4.1	4.1	4.1	4.1	3.6	3.7	3.9	3.9	77.0859	82.8000	74.3649	79.8069	159.3499	166.4248	156.9008	164.5200

The interaction of rare gas atoms were considered for four different sites – atop atom, bridge, 3-fold hollow and 3-fold filled sites – on the Cu (110) surface. Fig. 1 shows the 3 layer cluster model of Cu(111) surface and the sites mentioned. Single He, Ne, Ar and Kr atoms were brought above these surfaces and their distances are shown. Bridge site is on top of midpoint of AE. Atop atom site is above A or E.

The equilibrium Rg-metal surface bond distance (in Å) and binding energy (in meV) are presented in Table 1. We present the interaction energy curve as a function of metal-Rg distance for all the sites for Ar and Kr on Cu(111) as shown in Fig. 2. Curves for the other atoms are given in Supplementary Information with this paper. The total interaction energy is the sum of short and long range interactions and hence a minimum is expected for each pair of metal-Rg system. In general, the short-range interaction energy consists of various parts, as, electrostatic, hybridisation effect, many-body repulsions and kinetic repulsion energies, and is rather repulsive till the equilibrium is reached for each system. For the higher rare gas atoms, this is due to the overlap between the occupied levels of Rg atoms and the metal wave-functions which gives rise to a high repulsive kinetic energy. After the equilibrium distance is reached, the hybridisation and the many-body effects overcome the repulsive kinetic energy and result in an attractive interaction. For He, the atop site is the most stable with binding energy of 2.7309 meV, while the filled site follows closely (2.6309 meV). The bridged site also has almost same interaction energy (2.6109 meV) as the filled one. He is the least stable above the hollow site (2.5309 meV). The equilibrium distance remains the same for the filled, atop as well as hollow sites but increases to 3.5 A as we move on to the bridged site. This trend is somewhat different for Ne. The bridge site is the most stable (6.1580 meV) of the four adsorption sites. In contrast to that observed for He, the stability of the hollow site (5.8880 meV) is almost same as that of the filled one (5.8080 meV). The atop site, which was the most stable in case of He, is found to be the least stable adsorption site for Ne (5.4680 meV). The equilibrium distance is same (3.3 A) for bridge, filled and hollow sites. For the heavier rare gas atoms Ar and Kr, the trend of preferential adsorption site is completely different. For both Ar and Kr, the bridged site is found to be the most stable adsorption site. The binding energies obtained are 7.6684 meV and 6.1160 meV respectively. The

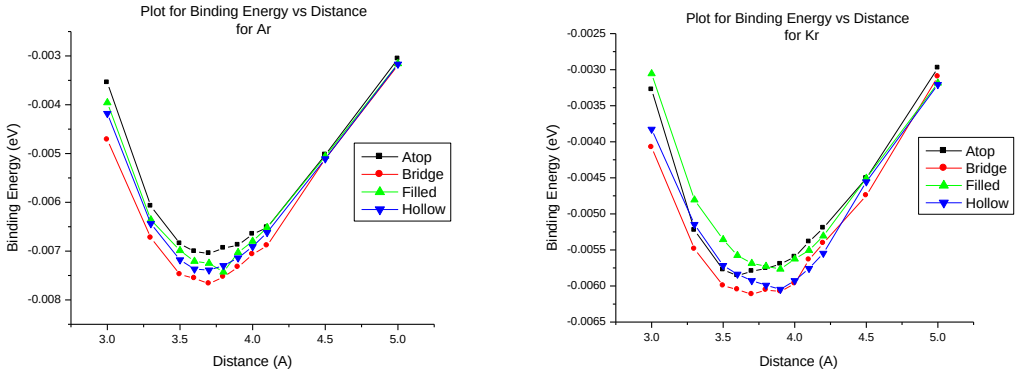

Fig. 2. Binding Energy plots of argon and krypton on Cu (111) for different sites.

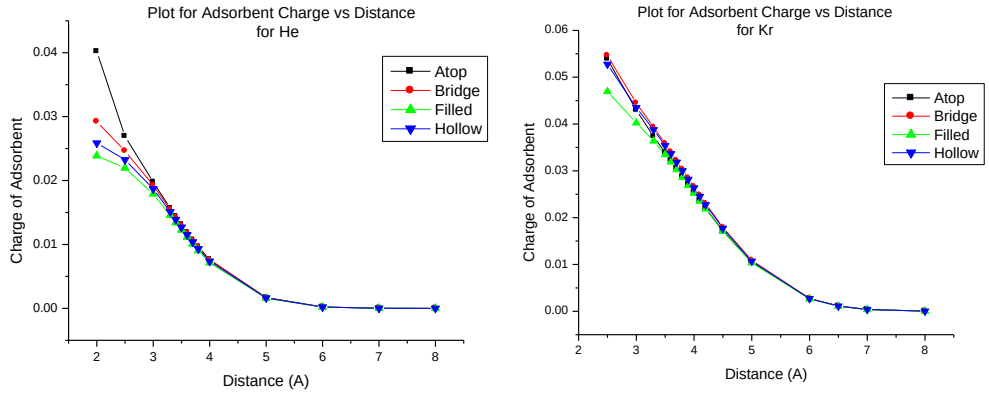

Fig 3. Plot of charge of the Rg atom in four different sites for He and Kr.

filled site follows closely for Ar with interaction energy 7.4284 meV. The atop and the filled site is observed as the least stable adsorption site for Ar (7.0484 meV) and Kr (5.6860 meV respectively). The binding energy values were corrected for basis set superposition error (BSSE). The BSSE values calculated by the method of Boys and Handy were found to be of the order of 10^{-5} eV, and hence were neglected.

We represent the charge of adsorbent rare gas atoms as a function of the metal-Rg distance for all adsorption sites in Fig 3. The results for He and Kr are shown; Ne behaves like He and Ar behaves like Kr on the Cu curface. The latter curves are given in Supplementary Information. The Lowdin charges are shown as they are considered superior to Mulliken charges, especially where not very highly polar systems are considered[50-52], and a specific trend is observed for all the adsorption sites. The charges of the adsorbent rare gas atoms decreases as the distance between the metal surface and the Rg atoms increase. The charge decreases rapidly upto distance of 4.0 A. At distances higher than 4.0 A, the charges decay exponentially and tend to zero as we further extrapolate the curve to a distance greater than 8.0 A. Except for the He adsorbent, all three other adsorbents have their highest charge for the filled sites. For He as adsorbent, the atop site possesses the maximum charge as compared to the other three. We also represent the charge of the three layers of the copper surface vs. metal-Rg distance for all sites in Fig. 4. Results for He and Kr are shown. Other results are given in Supplementary Information. Behaviour of Ne and Ar on copper are similar to that of He and Kr respectively. The heavier Rg atoms have different effect on copper surface as compared to the lighter atoms. For He and Ne, the Lowdin charges vary exponentially with metal-Rg atom distance, and maximum charge accumulation is found in the filled site. On the other hand, for Ar and Kr, the charge density initially increases steeply with the metal-Rg distance, and at a distance > 3.2 A, the curve assumes an exponential pattern. For the second layer, the charge density distribution pattern

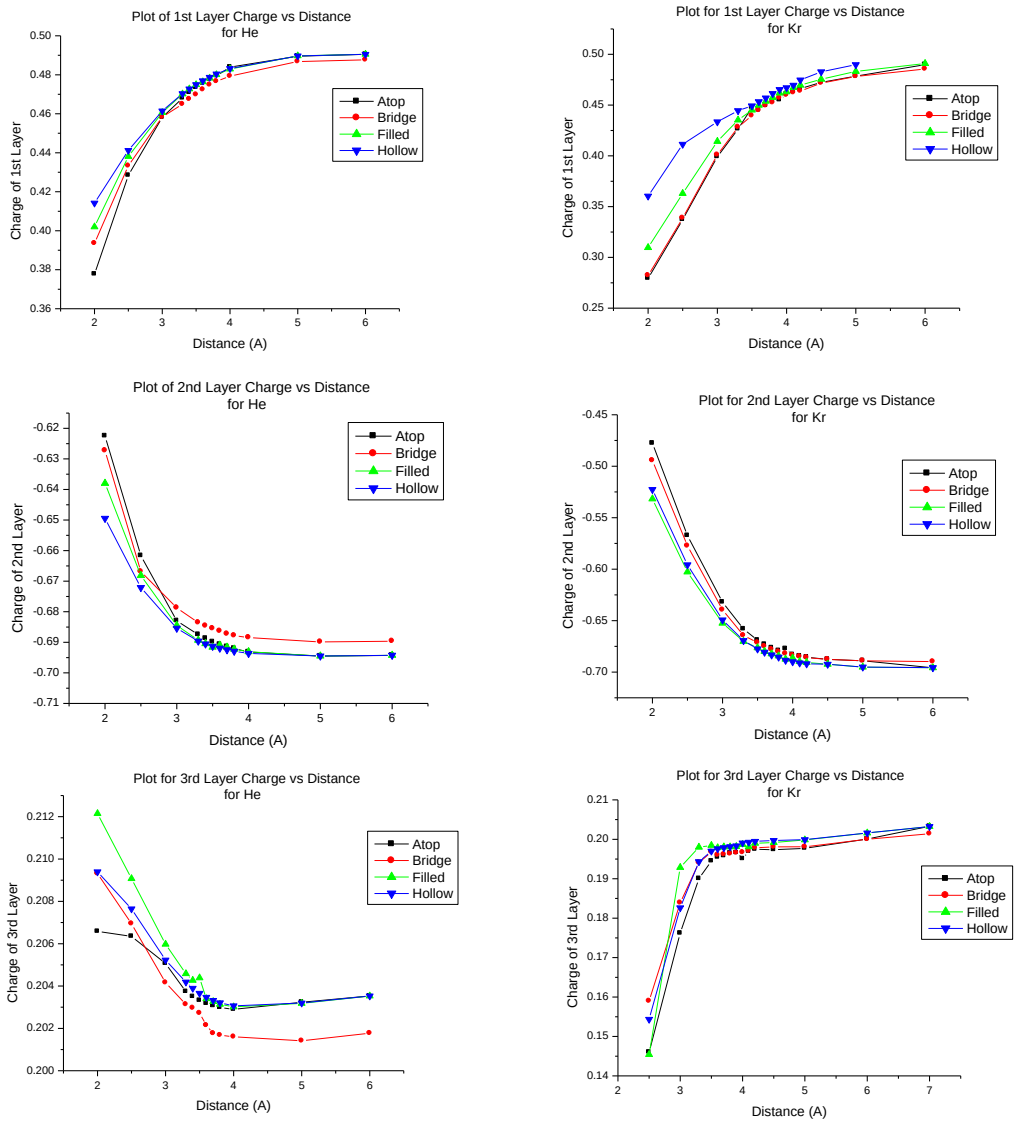

Fig. 4. Plot for charge on various layers of Cu surface for all sites for He and Kr.

is similar for all the adsorbents. The charge decreases exponentially and the rate of decrease is more pronounced as we move on to the heavier adsorbents. In case of the third layer, no pronounced change is observed for the lighter atoms. As we move to Ar and Kr, the charge slowly rises exponentially with distance. Note that charge on the second layer is negative, while those on the 1st and 3rd layers are positive. This is an instance of Friedel type oscillations, observed on the surface of a polarisable medium, when a charge is brought near the surface. Here, the Rg atom plays the part of the latter.

In Fig. 5 (a) – (b), we present the energies of the highest occupied molecular orbital (HOMO) and the lowest unoccupied molecular orbital (LUMO) energies of the metal-Rg system as a function of the distance between the above two. Please note that in standard MO theory, these represent the first ionization energy and the electron affinity values[53]. Both the HOMO and LUMO energies are found to represent an exponentially decaying curve for all the adsorption sites irrespective of the adsorbents. The HOMO energy however falls more sharply than that of the LUMO. Same trend is obtained for the dipole moments of the system for all sites. A sharp decrease is observed in the dipole moment values

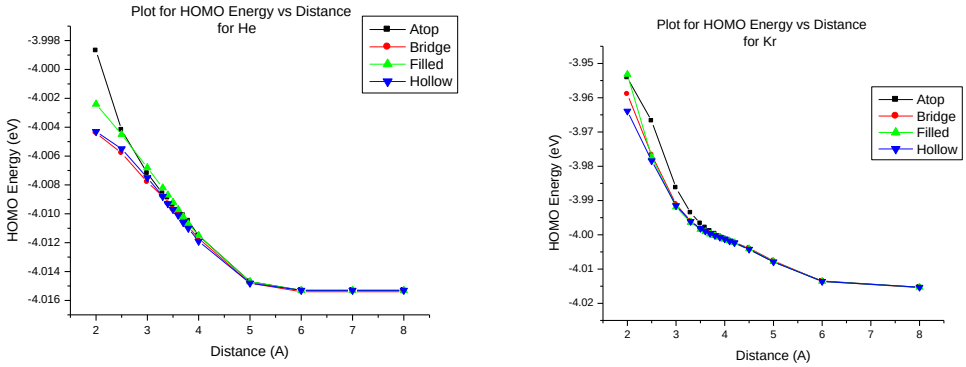

Fig. 5 (a). Plot of HOMO energy for four different sites for He and Kr.

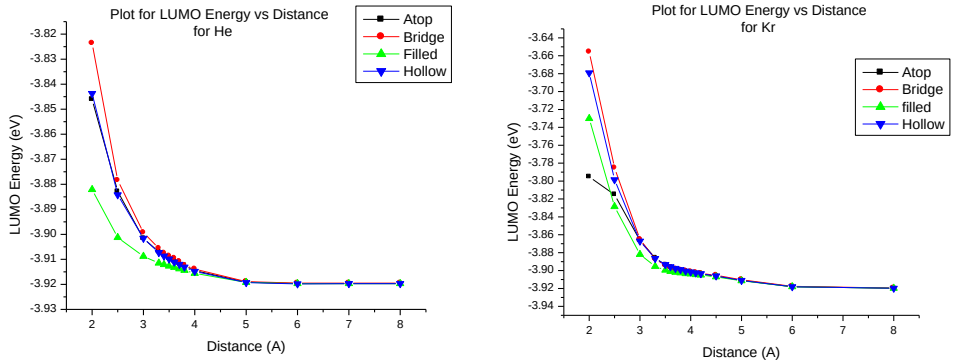

Fig 5 (b). Plot of LUMO energy for four different sites for He and Kr.

(Fig. 6) as the distance between the metal surface and the adsorbent atom increases. The dipole moment increases as the size of the adsorbent atom increases. We calculated global elctronegativity and hardness of the metal-adsorbent pairs for the four sites according to the method of Chattaraj et al[54] and the respective plots are shown in Fig. 6(a) – (c). All other adsorbents show sharp rise in electronegativity around the equilibrium metal-Rg distance and then assumes an exponential nature and after 5.0 A, remains more or less unchanged. The initial rise in electronegativity is more pronounced for the heavier atoms vis-a-vis He and Ne. On the other hand, the hardness of the system shows an exponential decrease uniformly for all the adsorbents. From the hardness and electronegativity values, we calculated the global electrophilicity of the system. In general, the plot of electrophilicity against metal-Rg distance shows rise in the above physical property. For He, the rise is exponential, but as we move on to Ne and Ar, the electrophilicity increases more sharply and finally for Kr, the curve shows extremely sharp nature, and assumes exponential nature only after 4.0 A.

Plots of HOMO of Ar at minimum energy configuration over the bridge site (Fig. 8 (a)) and at a much larger distance (8.0 A, Fig. 8 (b)) show the overlap with metal (surface) electrons in the former case, and no interaction in the latter. This behaviour is typical of all the systems studied, and is the origin of noble gas – metal interactions, as acknowledged by other workers[55-56,2]. The extent of overlap would determine polarization of the electron cloud and thus the properties displayed above.

In a detailed study of Xe-M-X systems (M = Au, Ag, Cu; X = F, Cl, Br) involving CCSD(T) and DFT calculations, with triple zeta basis and four different density functionals, Fang and Zhang[55] found correlations between electronegativity of halogen atoms and M-X bond lengths, HOMO-LUMO gap, Xe-M bond energy and electronic structure. The correlations in the first three cases come out as linear. What is interesting is that the values of these parameters in their work agree closely with ours.

In Fig. 9 (a), the density of states (DOS)[56] of He atom at its equilibrium position on the copper cluster is presented, along with that of the bare

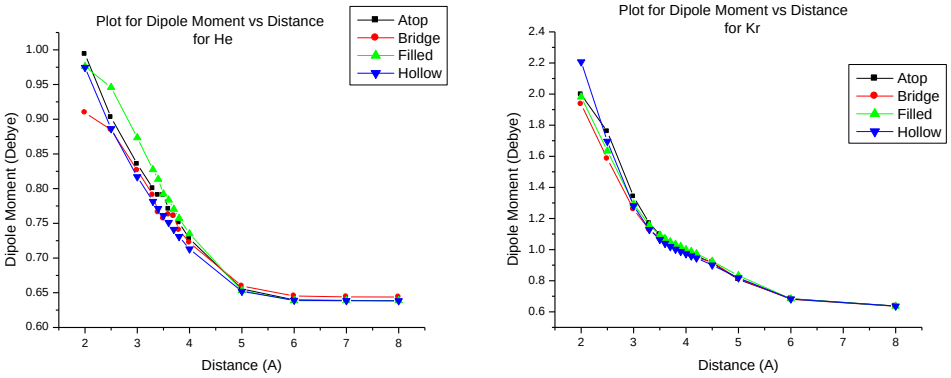

Fig 6. Plot of dipole moment for all sites for He and Kr

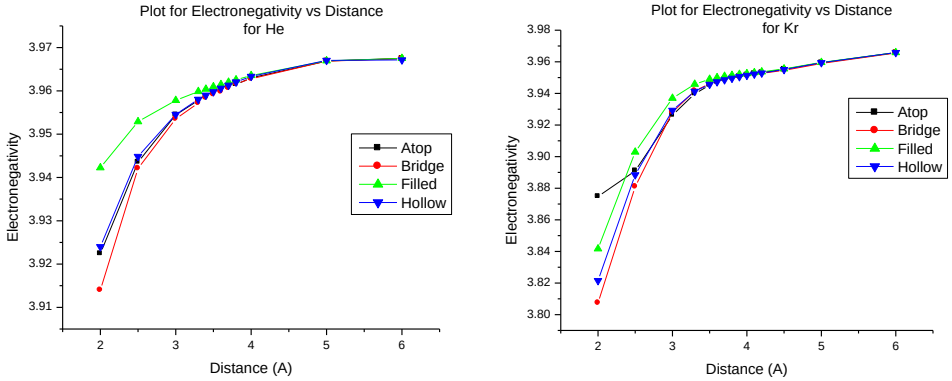

Fig. 7 (a). Plot of global electronegativity for all sites for He and Kr.

copper cluster. The two curves are virtually indistinguishable. This is in contrast to Fig. 9 (b), where Kr takes the place of helium. Clearly, the two DOS differ between -7 and -8 a.u., between -2 and -4 a.u. and near and beyond 0 a.u. (the Fermi level i.e. HOMO is at -0.151 a.u.). The new hump near -8 a.u. must indicate bonding between adsorbate and the metal. Here, we expected that He, being the lightest rare gas atom would make the least effect, and Kr being the heaviest one studied would have the largest effect on the DOS of the substrate, as has been borne out in the two figures. Other DOS curves may be found in Supplementary Information.

While there is no clear understanding of finer intricacies of interaction of rare-gas atoms with metal surfaces, there exist models where the metal electrons are treated as free, and local exchange-correlation functional was used to describe the interaction between the two species[2,57]. In these classic papers, the conclusion was that the local density functional was able to provide a good description to the rare-gas and metal interaction. However, it has also been shown elsewhere that

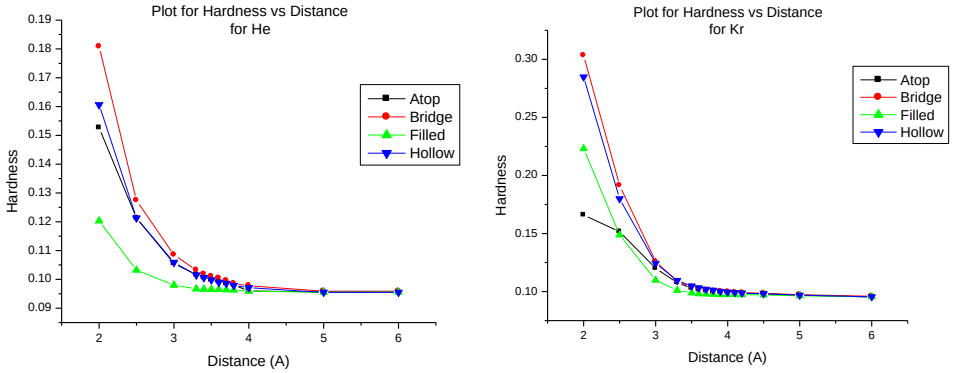

Fig. 7 (b). Plot of global hardness for all sites for He and Kr.

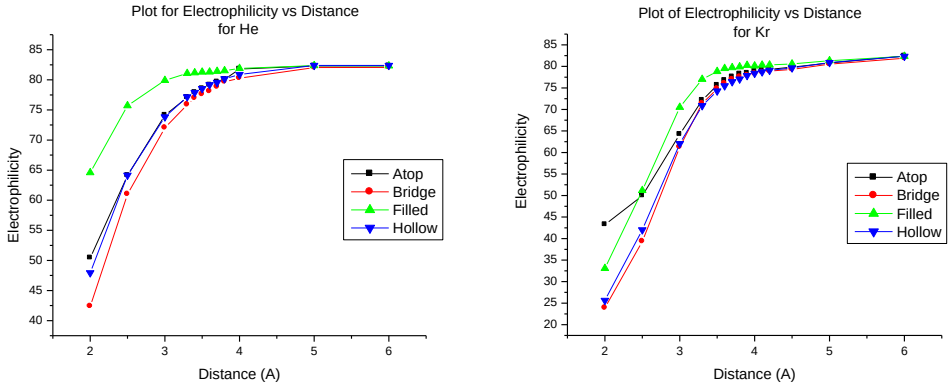

Fig. 7 (c). Plot of global electrophilicity for all sites for He and Kr.

only a nonlocal density functional can provide an effective description to such vanderwaals type interactions[58-61]. Evidently, much further work needs to be done on such systems.

CONCLUSION

We present a detailed study of rare gas atoms on a model 3-layer Cu(111) surface consisting of 26 atoms. The nature of interaction, when a rare gas atom approaches the surface, is the main focus of the study; interaction energy curves and related data e.g. minimum equilibrium distances are also presented. We present interaction of surface and atoms in four different sites viz., atop, bridge, filled and hollow sites. The nature of interaction of different single rare gas atoms for these sites was found to be different in each case. Except for He, bridge site was found to be the most favourable for adsorption. For He, atop site is the most stable one. Some other parameters of the above interactions were also considered viz. total charge of the adsorbent as a whole, and various layers of it separately, dipole moment, HOMO and LUMO energies, electrophilicity, hardness and electronegativity. These were considered as functions of rare gas atom-Cu surface distance. The charges of the 1st layer show sharp and then gradual exponential change with Rg-Cu distance; those of 2nd and 3rd layers are less pronounced. Charge variation of the 3rd layer is the flattest i.e. least affected. Dipole moments, hardness, HOMO and LUMO energies, adsorbent charge variations show regular exponential decrease with distance. Finally, the DOS of the adsorbate-substrate complex shows differences with that of the bare substrate, especially as the rare gas atom becomes more polarisable, at small regions deep in energy, but quite clearly near the Fermi level and beyond.

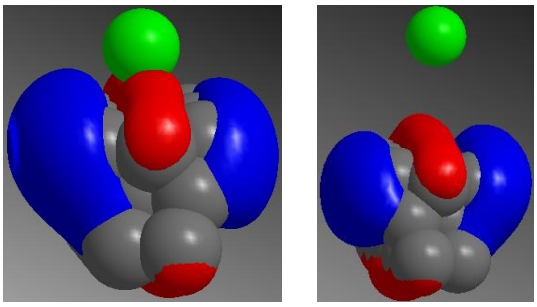

Fig. 8. HOMO of Ar atom (green) over bridge site of copper cluster at (a) equilibrium distance (4 A) and at (b) far away (8 A). Phases of the wavefunction are shown in red and blue.

Overall, in all the studies of various physical properties of the system, the bridged site shows the most pronounced effects, and hence can be considered as the most significant site for rare gas adsorption in Cu(111)-Rg atom system. For the lighter atoms, the changes are sharper, while for Ar and Kr, the plots assume somewhat flatter nature. The entire study was carried out considering a single rare gas atom approaching the metal surface. The study of the same system in presence of another similar or dissimilar Rg atom in an adjacent site may be of considerable interest, and is being carried out in our laboratory.

ACKNOWLEDGEMENT

The authors would like to acknowledge computational support received from the laboratory of Prof. S. K. Pati, JNCASR, Bangalore and Central Computing Facility, Dept. of Chemistry, KU provided under a DST-FIST grant.

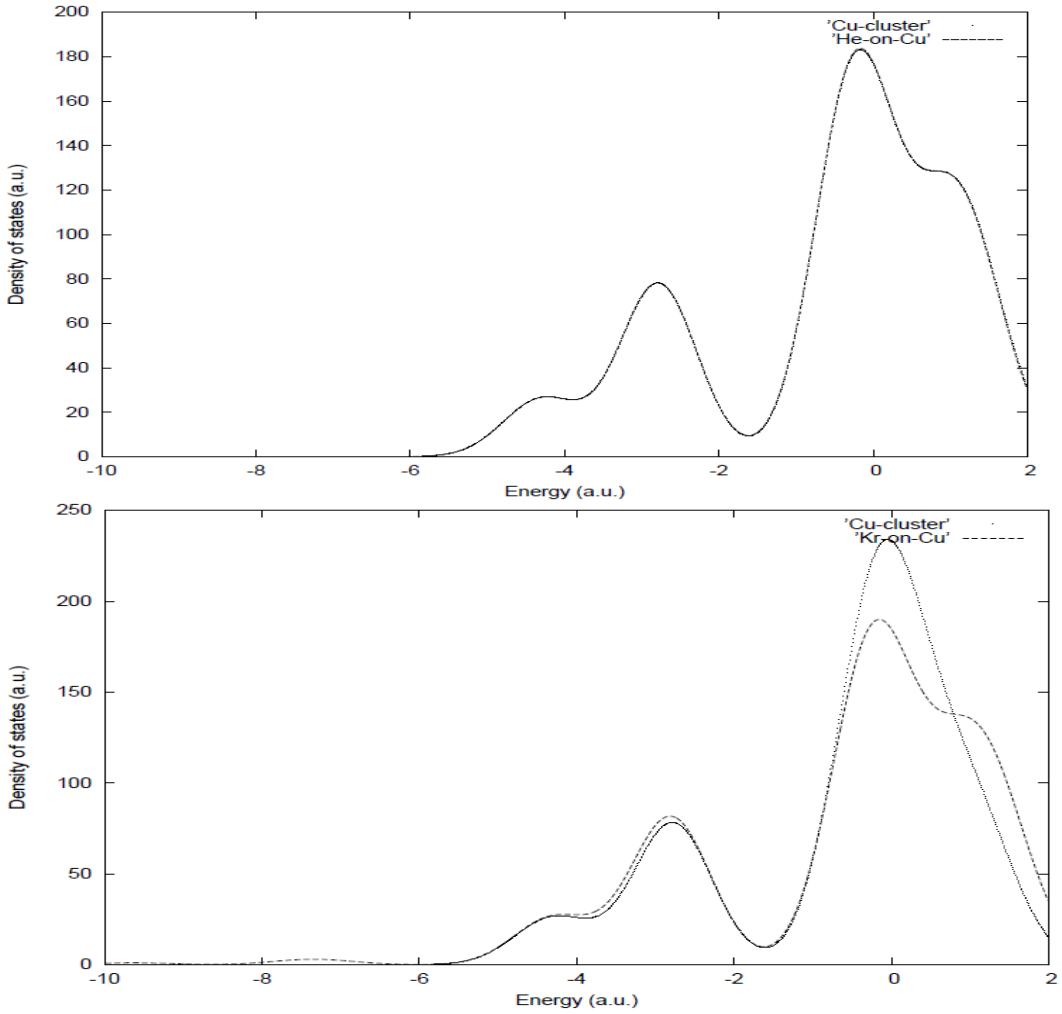

Fig. 9 (a) (above). DOS of bare copper cluster (dotted lines) and that of He on an atop-atom site on copper cluster (broken lines). See text for details.
Fig. 9 (b) (below). DOS of bare copper cluster (dotted lines) and that of Kr on an atop-atom site on copper cluster (broken lines). See text for details.

REFERENCES

[1] Schram A. in F. Ricca (Ed.). Adsorption-Desorption Phenomena. London: A Academic Press. 1992; 57.

[2] Lang ND. Interaction between Closed-Shell Systems and Metal Surfaces. Physical Review Letters [Internet]. American Physical Society (APS); 1981 Mar 30;46(13):842–5. Available from: http://dx.doi.org/10.1103/physrevlett.46.842

[3] Bruch LW, Cole MW, Zaremba E. Physical Adsorption: Forces and Phenomena. New York, Oxford University Press. 1997.

[4] Farias D, Rieder K-H. Atomic beam diffraction from solid surfaces. Reports on Progress in Physics [Internet]. IOP Publishing; 1998 Dec 1;61(12):1575–664. Available from: http://dx.doi.org/10.1088/0034-4885/61/12/001

[5] Sinha SK. (Ed). Ordering in Two Dimensions, North-Holland, Amsterdam. 1980.

[6] Wandelt K, Hulse JE. Xenon adsorption on palladium. I. The homogeneous (110), (100), and (111) surfaces. J Chem Phys [Internet]. AIP Publishing; 1984;80(3):1340. Available from: http://dx.doi.org/10.1063/1.446815

[7] Moog ER, Webb MB. Xenon and krypton adsorption on palladium (100). Surface Science [Internet]. Elsevier BV; 1984 Dec;148(2-3):338–70. Available from: http://dx.doi.org/10.1016/0039-6028(84)90586-7

[8] Vogt B, Kessler B, Müller N, Schönhense G, Schmiedeskamp B, Heinzmann U. Spin-resolved photoemission from Xe on Pd(111) in the dilute phase: The model case of singly adsorbed atoms.

Physical Review Letters [Internet]. American Physical Society (APS); 1991 Sep 2;67(10):1318–21. Available from: http://dx.doi.org/10.1103/physrevlett.67.1318

[9] Kern K, David R, Zeppenfeld P, Comsa G. Registry effects in the thermodynamic quantities of Xe adsorption on Pt(111). Surface Science [Internet]. Elsevier BV; 1988 Jan;195(3):353–70. Available from: http://dx.doi.org/10.1016/0039-6028(88)90347-0

[10] Barker JA, Rettner CT. Accurate potential energy surface for Xe/Pt(111): A benchmark gas/surface interaction potential. J Chem Phys [Internet]. AIP Publishing; 1992;97(8):5844. Available from: http://dx.doi.org/10.1063/1.463743

[11] Weiss PS, Eigler DM. Adsorption and accommodation of Xe on Pt{111}. Physical Review Letters [Internet]. American Physical Society (APS); 1992 Oct 12;69(15):2240–3. Available from: http://dx.doi.org/10.1103/physrevlett.69.2240

[12] Zeppenfeld P, Horch S, Comsa G. Interaction of xenon at surface steps. Physical Review Letters [Internet]. American Physical Society (APS); 1994 Aug 29;73(9):1259–62. Available from: http://dx.doi.org/10.1103/physrevlett.73.1259

[13] Wang S.C, Ehrlich G. Interaction of xenon at surface steps. J Chem Phys. 1991; 94:4071-4

[14] Sanders DE, DePristo AE. Metal/metal homo-epitaxy on fcc (001) surfaces: Is there transient mobility of adsorbed atoms? Surface Science [Internet]. Elsevier BV; 1991 Aug;254(1-3):341–53. Available from: http://dx.doi.org/10.1016/0039-6028(91)90666-g

[15] Unguris J, Bruch LW, Moog ER, Webb MB. Xe adsorption on Ag(111): Experiment. Surface Science. 1979 Aug;87(2):415–36. Available from: http://dx.doi.org/10.1016/0039-6028(79)90539-9

[16] Bruch LW, Unguris J, Webb MB. Effects of lateral compression on a non-registered monolayer. Surface Science. 1979 Aug;87(2):437–56. Available from: http://dx.doi.org/10.1016/0039-6028(79)90540-5

[17] Unguris J, Bruch LW, Moog ER, Webb MB. Ar and Kr adsorption on Ag(111). Surface Science. 1981 Sep;109(3):522–56. Available from: http://dx.doi.org/10.1016/0039-6028(81)90425-8

[18] M Black JE, Bopp P. Orientation of small rafts of xenon atoms physisorbed on Pt(111): A molecular-dynamics study. Physical Review B. 1986 Nov 15;34(10):7410–2. Available from: http://dx.doi.org/10.1103/physrevb.34.7410

[19] Kern K, David R, Palmer RL, Comsa G. Complete wetting on "'strong'" substrates: Xe/Pt(111). Physical Review Letters. 1986 Jun 30;56(26):2823–6. Available from: http://dx.doi.org/10.1103/physrevlett.56.2823

[20] Kern K, David R, Palmer RL, Comsa G. The Novaco-McTague rotated Xe monolayer on Pt(111): A high-order commensurate locked phase. Applied Physics A Solids and Surfaces. 1986 Sep;41(1):91–3. Available from: http://dx.doi.org/10.1007/bf00618537

[21] Kern K, David R, Palmer RL, Comsa G. Thermodynamic measurements of Xe-Adsorptton on Pt(111). Surface Science. 1986 Sep;175(1):L669–L674. Available from: http://dx.doi.org/10.1016/0039-6028(86)90072-5

[22] Kern K, David R, Zeppenfeld P, Palmer R, Comsa G. Symmetry breaking commensurate-incommensurate transition of monolayer Xe physisorbed on Pt(111). Solid State Communications. 1987 May;62(6):391–4. Available from: http://dx.doi.org/10.1016/0038-1098(87)91040-4

[23] Kern K. Symmetry and rotational epitaxy of incommensurate Xe layers on Pt(111). Physical Review B. 1987 May 15;35(15):8265–8. Available from: http://dx.doi.org/10.1103/physrevb.35.8265

[24] Morrison JA, Los JM, Drain LE. The heat capacity, integral heat of adsorption and entropy of argon adsorbed on titanium dioxide. Transactions of the Faraday Society. 1951;47:1023. Available from: http://dx.doi.org/10.1039/tf9514701023

[25] Drain LE, Morrison JA. Interpretation of the thermodynamic properties of adsorbed argon at low surface coverages. Transactions of the Faraday Society. 1952;48:316. Available from: http://dx.doi.org/10.1039/tf9524800316

[26] Drain LE, Morrison JA. Thermodynamic properties of argon adsorbed on rutile. Transactions of the Faraday Society. 1952;48:840. Available from: http://dx.doi.org/10.1039/tf9524800840

[27] Gomes J.R.B, Prates Ramalho JP. Adsorption of Ar atoms on the relaxed defect-free Ti O 2 (110) surface. Phys Rev B. 2005; 71:235421-8

[28] Gomes JRB, Ramalho JPP, Illas F. Adsorption of Xe atoms on the TiO2(110) surface: A density functional study. Surface Science. 2010 Feb;604(3-4):428–34. Available from: http://dx.doi.org/10.1016/j.susc.2009.12.009

[29] Black JE, Janzen A. Persistent and non-persistent uniaxial strain events observed in small rafts of xenon physisorbed on Pt(111): A molecular dynamics study. Surface Science. 1989 Jul;217(1-2):199–232. Available from: http://dx.doi.org/10.1016/0039-6028(89)90544-x

[30] Black JE, Janzen A. A molecular dynamics of small rafts of xenon physisorbed on platinum(111). Langmuir. 1989 May;5(3):558–62. Available from: http://dx.doi.org/10.1021/la00087a003

[31] Black JE, Janzen A. Uniaxial strain events in molecular-dynamics simulations of small rafts of xenon physisorbed on Pt(111). Physical Review B. 1988 Oct 15;38(12):8494–6. Available from: http://dx.doi.org/10.1103/physrevb.38.8494

[32] Black JE, Janzen A. Transition from commensurate to incommensurate xenon rafts on platinum (111) observed with molecular dynamics. Physical Review B. 1989 Mar 15;39(9):6238–40. Available from: http://dx.doi.org/10.1103/physrevb.39.6238

[33] Bethune DS, Barker JA, Rettner CT. Calculation of desorption rates for Xe/Pt(111) using a realistic gas–surface potential. J Chem Phys. 1990;92(11):6847. Available from: http://dx.doi.org/10.1063/1.458271

[34] Arumainayagam CR, Madix RJ, Mcmaster MC, Suzawa VM, Tully JC. Trapping dynamics of xenon on Pt(111). Surface Science. 1990 Feb;226(1-2):180–90. Available from: http://dx.doi.org/10.1016/0039-6028(90)90164-4

[35] Tully JC. Stochastic-trajectory simulations of gas–surface interactions: Xe on Pt(111). Faraday Discuss Chem Soc. 1985;80(0):291–8. Available from: http://dx.doi.org/10.1039/dc9858000291

[36] Tully JC. Dynamics of gas-surface interactions: Thermal desorption of Ar and Xe from platinum. Surface Science. 1981 Nov;111(3):461–78. Available from: http://dx.doi.org/10.1016/0039-6028(81)90402-7

[37] Grimmelmann EK. Molecular dynamics of infrequent events: Thermal desorption of xenon from a platinum surface. J Chem Phys. 1981;74(9):5300. Available from: http://dx.doi.org/10.1063/1.441696

[38] Hall B, Mills DL, Zeppenfeld P, Kern K, Becher U, Comsa G. Anharmonic damping in rare-gas multilayers. Physical Review B. 1989 Sep 15;40(9):6326–38. Available from: http://dx.doi.org/10.1103/physrevb.40.6326

[39] Gottlieb JM. Energy and structure of uniaxial incommensurate monolayer solids: Application to Xe/Pt(111). Physical Review B. 1990 Sep 15;42(8):5377–80. Available from: http://dx.doi.org/10.1103/physrevb.42.5377

[40] Gottlieb JM, Bruch LW. Uniaxial incommensurate rare-gas-monolayer solids. II. Application to Xe/Pt(111). Physical Review B. 1991 Sep 15;44(11):5759–65. Available from: http://dx.doi.org/10.1103/physrevb.44.5759

[41] Eigler DM, Weiss PS, Schweizer EK, Lang ND. Imaging Xe with a low-temperature scanning tunneling microscope. Physical Review Letters. 1991 Mar 4;66(9):1189–92. Available from: http://dx.doi.org/10.1103/physrevlett.66.1189

[42] Potthoff M, Hilgers G, Müller N, Heinzmann U, Haunert L, Braun J, et al. Structure investigations of Xe-adsorbate layers by spin-polarized low-energy electron diffraction I. () R30°-Xe/Pt (111). Surface Science. 1995 Jan;322(1-3):193–206. Available from: http://dx.doi.org/10.1016/0039-6028(95)90030-6

[43] Hilgers G, Potthoff M, Müller N, Heinzmann U. Structure investigations of Xe-adsorbate layers by spin-polarized low-energy electron diffraction II. (√3 × √3) R30°-Xe/Pd (111) and the "dilute" phase of Xe/Pd(111). Surface Science. 1995 Jan;322(1-3):207–20. Available from: http://dx.doi.org/10.1016/0039-6028(95)90031-4

[44] Pérez R, García-Vidal FJ, de Andrés PL, Flores F. Adsorption of xenon on metals: a theoretical analysis. Surface Science. 1994 Apr;307-309:704–9. Available from: http://dx.doi.org/10.1016/0039-6028(94)91480-x

[45] Perdew JP, Wang Y. Accurate and simple analytic representation of the electron-gas correlation energy. Physical Review B. 1992 Jun 15;45(23):13244–9. Available from: http://dx.doi.org/10.1103/physrevb.45.13244

[46] Becke AD. A new mixing of Hartree–Fock and local density-functional theories. J Chem Phys. 1993;98(2):1372. Available from: http://dx.doi.org/10.1063/1.464304

[47] Perdew JP, Burke K, Ernzerhof M. Generalized Gradient Approximation Made Simple. Physical Review Letters. 1996 Oct 28;77(18):3865–8. Available from: http://dx.doi.org/10.1103/physrevlett.77.3865

[48] Schäfer A , Horn H, Ahlrichs R. Fully optimized contracted Gaussian basis sets for atoms Li to Kr. J Chem Phys. 1992;97(4):2571. Available from: http://dx.doi.org/10.1063/1.463096

[49] Neese F. ORCA– an ab-initio, Density Functional and Semiempirical program package, Version 2.8, University of Bonn. 2010.

[50] Mayhall NJ , Raghavachari K, Hratchian HP. ONIOM-based QM:QM electronic embedding method using Löwdin atomic charges : Energies and analytic gradients. J Chem Phys. 2010;132(11):114107. Available from: http://dx.doi.org/10.1063/1.3315417

[51] Gross KC, Seybold PG, Hadad CM. Comparison of different atomic charge schemes for predicting pKa variations in substituted anilines and phenols. International Journal of Quantum Chemistry. 2002;90(1):445–58. Available from: http://dx.doi.org/10.1002/qua.10108

[52] Lewars EG. Computational Chemistry. 2nd ed.Heidelberg. 2011; 429.

[53] Pilar FL. Elementary Quantum Chemistry, 2nd ed. New York: McGraw Hill; 1990; 278.

[54] Chattaraj PK, Sarkar U, Roy DR. Electrophilicity Index. Chem Rev. 2006 Jun;106(6):2065–91. Available from: http://dx.doi.org/10.1021/cr040109f

[55] Fang H, Zhang X-G. Density functional study on rare gas-noble metal closed-shell interaction in XeMX (M = Au, Ag, Cu; X = F, Cl, Br) systems. Theoretical Chemistry Accounts. 2009 Mar 17;123(5-6):443–53. Available from: http://dx.doi.org/10.1007/s00214-009-0555-7

[56] The density of states (DOS) was constructed from the eigenvalue spectrum of each system by considering a set of Gaussian functions centered on the eigenvalues with a small finite spread. Lorentzian functions were found to give very similar spectra.

[57] Lang ND, Williams AR. Theory of local-work-function determination by photoemission from rare-gas adsorbates. Physical Review B. 1982 Feb 15;25(4):2940–2. Available from: http://dx.doi.org/10.1103/physrevb.25.2940

[58] Grimme S. Accurate description of van der Waals complexes by density functional theory including empirical corrections. Journal of Computational Chemistry. 2004;25(12):1463–73. Available from: http://dx.doi.org/10.1002/jcc.20078

[59] Grimme S. Semiempirical GGA-type density functional constructed with a long-range dispersion correction. Journal of Computational Chemistry. 2006;27(15):1787–99. Available from: http://dx.doi.org/10.1002/jcc.20495

[60] Jurečka P , Černý J , Hobza P, Salahub DR. Density functional theory augmented with an empirical dispersion term. Interaction energies and geometries of 80 noncovalent complexes compared with ab initio quantum mechanics calculations . Journal of Computational Chemistry. 2007 Jan 30;28(2):555–69. Available from: http://dx.doi.org/10.1002/jcc.20570

[61] Foster ME, Sohlberg K. Empirically corrected DFT and semi-empirical methods for non-bonding interactions. Phys Chem Chem Phys. 2010;12(2):307–22. Available from: http://dx.doi.org/10.1039/b912859j